PERGAMON

International Journal of Multiphase Flow 28 (2002) 1075–1090

International Journal of Multiphase Flow

www.elsevier.com/locate/ijmulflow

Turbulence modification by particles in a horizontal pipe flow

Camilla Ljus, Bert Johansson, Alf-Erik Almstedt *

Department of Thermo and Fluid Dynamics, Chalmers University of Technology, Hörsalsvägen 7, S-412 96 Göteborg, Sweden

Received 14 May 2000; received in revised form 8 February 2002

Abstract

Measurements were made of turbulence intensities and turbulent energy spectra in a fully developed, turbulent air–particle pipe flow. The influence of the particles on the turbulence was studied. Measurements were made with spherical particles and particles with a large aspect ratio (pulp fibres). There is a significant change in turbulence intensity at higher particle concentrations with loading ratios of $m = 0.1$ and 0.03. The measurements show that the turbulence intensity increases close to the centre of the pipe while the turbulence intensity decreases close to the pipe wall for the spherical particles. These results are in agreement with earlier measurements found in the literature. For the fibres, the turbulence intensity decreases over the whole pipe cross-section. Fibre flocs, however, give variations in the mean velocity that result in the production of turbulence in the lower part of the channel.

Keywords: Turbulence; Air–particle flow; Turbulence modification; Hot film; Measurements; Pipe flow

1. Introduction

Many types of particulate two-phase flows are affected by turbulence, e.g. mixing in bioreactors, the spreading of small particles in the atmosphere, transportation of particles through pipes and channels, separation in cyclones and sediment transport in rivers and oceans. Turbulence plays an important role in applications that involve the transport or mixing of particles. To improve the efficiency of these processes and the quality of the final products, it is necessary to understand and be able to control mechanisms that influence the flow field. Turbulence gives rise to the diffusion of particles, and the particles may affect the turbulence (two-way coupling). The presence of particles in turbulent fluid flow may alter the turbulence levels and the structure of the turbulence. Experimental work, e.g. by Tsuji and Morikawa (1982), Rashidi et al. (1990),

* Corresponding author. Tel.: +46-31-772-1407; fax: +46-31-180976.
E-mail address: affe@tfd.chalmers.se (A.-E. Almstedt).

0301-9322/02/$ - see front matter
PII: S0301-9322(02)00020-4

Kulick et al. (1994) and Kaftori et al. (1998) shows that particles may either increase or decrease the turbulence levels depending on the size of the particles. Small particles increase the dissipation of turbulent energy, and large particles may cause additional turbulent production. Particles of intermediate sized can have either effect depending on the part of the flow field that is studied. The length scale of the turbulence may also be affected since a redistribution of energy between different wave numbers can occur, cf., e.g. Tsuji et al. (1984) and Sato et al. (1995). The experimental results for energy spectra are, however, somewhat contradictory. Furthermore, most experimental investigations are made with spherical particles and not with large aspect ratio particles like pulp fibres.

Many attempts have been made to model turbulence modification phenomena numerically, cf., e.g. Dannon et al. (1977), Choi and Chung (1983), Elgobashi and Abou-Arab (1983), Pourahmadi and Humphrey (1983), Chen and Wood (1984) and Yokomine and Shimizu (1995). However, there is still room for improving the turbulence modelling of particulate two-phase flows. To be able to develop better turbulence models that capture correct turbulence behaviour in particulate flows, it is necessary to understand the two-way coupling between the particles and the turbulence. This experimental investigation was performed to improve the understanding of turbulence modification phenomena and to verify numerical calculations. The effect of particles on turbulence in a fully developed pipe flow has been studied, and the particles used are both spherical particles and large aspect ratio pulp fibres. Measurements of turbulence intensities and turbulent spectra were performed using a hot-film technique developed for measurements in gas flows, cf. Ljus et al. (2000).

2. Measuring technique

Turbulence measurements in two-phase flows are complicated in several ways. Laser–Doppler anemometry (LDA) is difficult to use in flows with pulp fibres or other opaque particles for which visibility decreases with the distance from the wall. It may also be difficult to separate signals coming from tracer particles and other larger particles. It is also complicated to calculate turbulence energy spectra since the sampling is not made at equidistant time intervals, cf., e.g. Tsuji and Morikawa (1982). Using a hot wire in gas–particle flows is impossible because of the fragile probe, and even ordinary hot film probes do not last long in such flows. To avoid the complications of LDA and get results using a simpler method a wedge-shaped hot-film probe was used. These kinds of probes have a poor frequency response in airflow, however, because of a non-negligible heat transfer to the substrate. One approach that can be used to overcome this problem is to perform a dynamic calibration, although this method requires a complicated shaking device. Here, a technique developed by Ljus et al. (2000) is used that makes it possible to use a static calibration of the probe. The method is based on the theoretical derivation of heat transfer in the substrate of a film probe by Bellhouse and Schulz (1967) and uses a correction function for the turbulence energy spectrum. The constants in the correction function are determined by comparing the turbulence energy spectra for the same flow case from a standard hot wire and the hot film. It is worth mentioning that these constants are probe dependent and that the correction function takes into account the mean velocity. After applying the correction function to the spectra measured with hot film in a particulate flow, the variance of the turbulence component

studied is determined by integrating the corrected spectrum. For further details, cf. Ljus et al. (2000).

When measurements with particles are performed, the particles that collide with the probe will give rise to occasional samples with an amplitude perhaps 10 times higher than the regular amplitude, cf. Fig. 15. These samples are very few compared with the total number of samples for the present dilute suspensions and can easily be removed by setting a maximum level of the fluctuating signal. This routine is in analogy with the sorting out of the so-called "bad samples" when turbulence measurements are made with LDA where a normal setting of the maximum level is three times the standard deviation. This threshold is also used in the present work.

3. Experimental set-up

The test rig consists of a 10-m long straight aluminium pipe with an inner diameter of 104 mm, connected to a sucking fan at the exit section, cf. Fig. 1. The inlet of the pipe is smoothly shaped to prevent separation. To ensure a fully developed flow, all the measurements are performed 9.0 in (87 diameters) downstream of the inlet. A micromanipulator makes it possible to position the probe with an accuracy of 0.05 mm. For the probe mounting, a removable pipe section is located 50 mm downstream of the measuring section. A classical Venturi tube with a machined convergent section with a diameter ratio of 0.75, designed according to the ISO 5167-1 standard, is mounted downstream of the removable section. At low-loading ratios, the Venturi can be used to measure the mass flow of air, $\dot{m}_g$, without a correction for the presence of particles, cf., e.g. Sharma and Crowe (1978) and Lee and Crowe (1982). There is also a Plexiglas section of the pipe to allow visual observation. The pipe exit is connected to the fan with a bellow to prevent vibrations from the fan from spreading to the pipe and to keep it electrically isolated from the fan. Pressure taps are mounted downstream and upstream of the measuring section to enable measurements of pressure drop for determination of the friction velocity, u^*.

The spherical particles are fed into the entrance of the pipe through a small Plexiglas pipe with a diameter of 50 mm, centred in the aluminium pipe, using a screw feeder. For the cases with pulp fibres, a mill is used to separate the fibres from a paper sheet into single fibres. The fibres are then fed into the pipe entrance through a bellow connected to the pipe.

The anemometer system used is a DANTEC 56C, and the analogue signals are digitized using a Macadios data acquisition card (12 bit AD converter, 4 channels sample and hold unit). In the

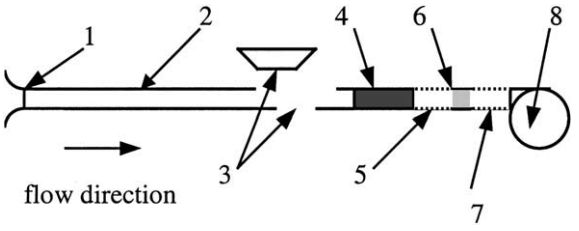

Fig. 1. Experimental test rig: 1. Smoothly shaped inlet section. 2. Aluminium pipe. 3. Removable pipe section. 4. Venturi tube. 5. Plexiglas section. 6. "étoile" straightener. 7. Bellow. 8. Fan.

present experiments, the sampling frequency is set to 10 kHz, the signal is low-pass filtered at 5 kHz and the number of samples are 409,600 for each run, which gives a total sampling time of 41 s.

When measurements are made with higher concentrations of pulp fibres, the fibres tend to form flocs, which may stick on the probe. Most of the smaller flocs will come loose after a short time, but some of the larger flocs, especially at the bottom wall, may stay on the probe. Therefore, in the measurements with fibres, the probe must be checked after each sampling run and cleaned if necessary. However, it is more difficult to discover smaller flocs that stay on the probe for a short time and come off before the sampling is completed. The intervals during the sampling where flocs have been stuck on the probe are, however, easily identified by examining the total signal. Signals from runs with and without flocs on the probe are shown in Fig. 2. The mean voltage changes level immediately when the floc collides with the probe and, when the floc comes loose, the mean voltage changes back to its original value. The parts of the signal where flocs have been stuck on the probe must be removed from the signal before the evaluation is made. The floc problem described here has slightly modified the measuring routines for the high concentration fibre case in the following way: the total number of samples are 51,200 for each run and the sampling time is 5 s. This is repeated 8–10 times so that the total sampling time is about 40 s, and the probe is cleaned of flocs before each run. This is done in order to get as many samples as possible before flocs become stuck on the probe and the signal becomes useless.

The probes are calibrated in a low-speed wind tunnel against a Pitot-static tube, and the calibration function suggested by Siddal and Davies (1972) is employed. Each sampled anemometer voltage is transferred to a velocity to avoid the linearization problem, and the velocity statistical properties are calculated using an in-house designed computer code. This procedure has been tested in several other experiments, cf., e.g. Löfdahl et al. (1992) and Abrahamsson et al. (1994). In the present experiments, however, the procedure is slightly modified since the correction method for the hot film frequency response is used. The variance of the fluctuating velocities is calculated by integration of the corrected energy spectrum, cf. Ljus et al. (2000). All Fast Fourier

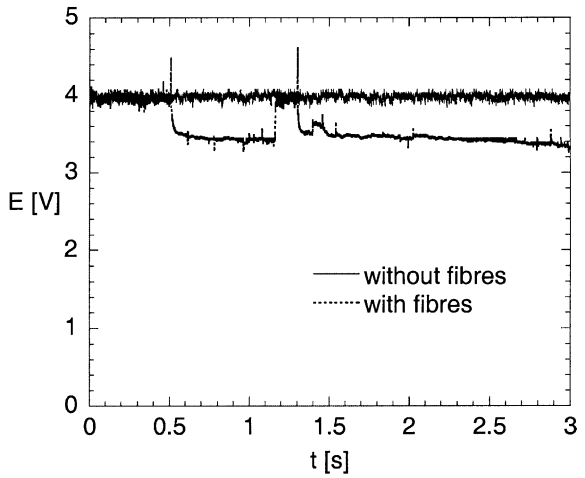

Fig. 2. Signals from runs with and without fibres. The signals almost coincide when there are no flocs of fibres stuck on the probe.

Transforms are calculated for a block size of 1024 samples, which gives a 9.8 Hz frequency resolution at a 10 kHz sampling frequency. When the total number of samples is 300,000–400,000 in every position measured, each energy spectrum is calculated as the averaged squared modulus of 300–400 independent FFTs. DANTEC's wedge-shaped film probe 55R31 is used for the measurements.

4. Measurements

To ensure that the flow without particles is a normal, fully developed turbulent pipe flow, measurements were made of the velocity profile and the profile of the stream-wise turbulent velocity component at a mean velocity of 19 m/s. Fig. 3 shows the dimensionless mean velocity profile, $u^+ = U/u^*$, as a function of the dimensionless wall distance, $y^+ = u^* y/v$. Here U is the local mean velocity in the streamwise direction, u^* is the friction velocity, y the wall distance and v the kinematic viscosity. The profile shows the logarithmic shape of a fully developed turbulent velocity profile. The constants in the log law are 2.44 and 5.2, which agree well with those suggested in the literature, cf., e.g., Tennekes and Lumley (1972). In the empirical equation for the velocity profile for a smooth pipe at high Reynolds numbers,

$$U/U_{\max} = (y/R)^{1/n}, \tag{1}$$

where $U_{\max}$ is the maximum velocity and R the pipe radius, the constant, n, is 7.34, cf. Fig. 4. This is in accordance with the constants given in Schlichting (1968). Fig. 5 shows the profile of the turbulence intensity, u'/u^*. The turbulence levels are in agreement with the approximate relation for the inertial sub-layer, $u' \approx 2u^*$, given by Tennekes and Lumley (1972).

Measurements were made with spherical polyacrylate particles with a size distribution of diameters between 100 and 800 μm (98%). Two different mean velocities, 12 and 19 m/s, were used

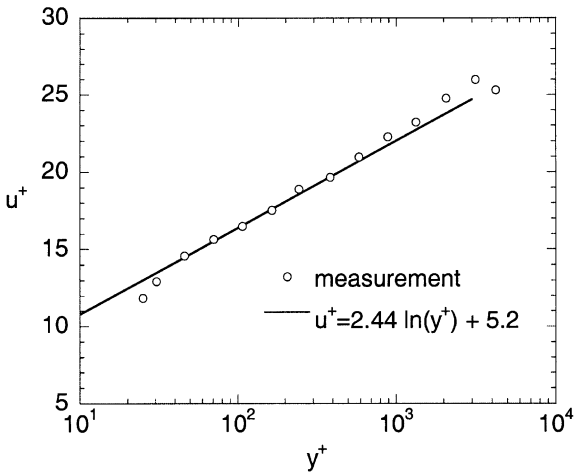

Fig. 3. Dimensionless mean velocity profile as a function of the dimensionless wall distance (inner scaling) for the unladen flow.

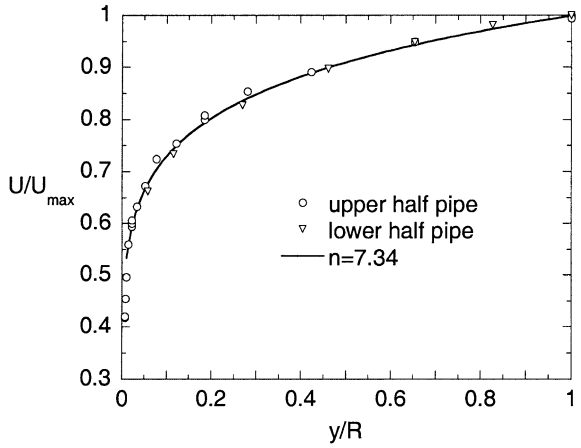

Fig. 4. Dimensionless mean velocity profile in outer scaling.

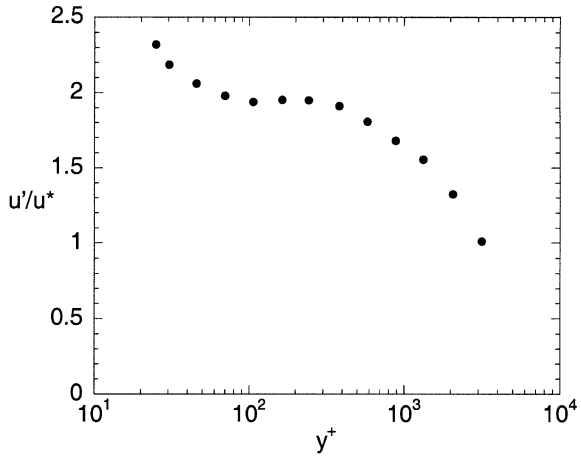

Fig. 5. Dimensionless turbulence intensity profile in inner scaling for the unladen flow.

and a loading ratio, i.e. the ratio between the massflow of the particles to the massflow of the air, $m = 0.1$. Measurements were also made with fibers of mechanical pulp at low-loading ratio, $m = 0.01$, at a velocity of 12 m/s and with fibres of chemical pulp at a loading ratio of $m = 0.03$ and a velocity of 19 m/s. The length of the fibres is about 3 mm and the aspect ratio is in the order of 50. The reason why the loading ratio is lower in the fibre cases than in the spherical particle cases is that floc forming makes measurement impossible at particle concentrations that are too high. However, even at this lower concentration of fibres there is a clearly visible effect on turbulence. It can also be noted that, for the fibre cases where flocs are formed, the concentration of single particles over the pipe cross-section will decrease along the pipe as the flocs are formed. The loading ratio presented here is the total loading ratio and does not say anything about the mass flow of flocs and single fibres, respectively. The distribution of fibres between flocs and single

Table 1
Summary of test cases

	Particle type	Particle density (kg/m^3)	Loading ratio	Gas mean velocity (m/s)	Re_d
Case 1	Spherical	1000	0.1	12	8.21×10^4
Case 2	Spherical	1000	0.1	19	1.30×10^5
Case 3	Fibre	1000	0.01	12	8.21×10^4
Case 4	Fibre	1000	0.03	19	1.30×10^5

fibres has not yet been studied. The response time of the spherical particles is about 0.5 s and that of the fibres is smaller, since the drag force on the fibres is larger. This indicates that the particle velocity has reached the terminal velocity, i.e. is approximately equal to the gas velocity, at the measuring section 9 m from the inlet. The different cases investigated are summarized in Table 1, where Re_d is the Reynolds number based on the pipe diameter.

5. Results

For the measurement with the spherical particles and a mean velocity of 12 m/s, i.e. case 1, the influence of the particles on the flow is significant. Fig. 6 shows the dimensionless gas velocity profile, $U/U_{\max}$, as a function of the dimensionless coordinate, $(y-R)/R$, where y is the vertical distance from the upper pipe wall for air–particle flow and for pure airflow. The figure shows that the velocity profile for the particle case is asymmetric and that the velocity in the lower part of the channel decreases when particles are added to the flow. The reason for this behaviour is of course that the particles are affected by gravity and the distribution of particles over the pipe cross-section is non-uniform. When the turbulence levels are not sufficiently high, the particles will accumulate at the bottom of the pipe. The gas velocity below the centreline decreases since

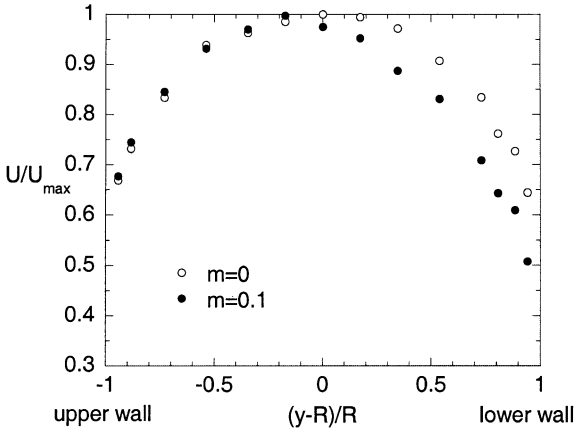

Fig. 6. Dimensionless mean velocity profiles for case 1 and for the unladen flow.

momentum is transferred from the gas phase to the particle phase. There are no experimental results of the distribution of particles over the cross-section, but calculations of the corresponding cases show that there is a significant increase of particle concentration in the lower part of the pipe, cf. Ljus and Almstedt (2001).

Fig. 7 shows the local turbulence intensity for the gas phase, u'/U, as a function of $(y-R)/R$ for the particle flow and the pure airflow. In the upper part of the pipe, where the particle concentration is low, the turbulence intensity is not affected by the particles. In the lower part, however, there is a significant effect on the turbulence intensity. In the middle section of the pipe below the centreline, the turbulence is enhanced by the particle presence, while turbulence is attenuated close to the lower wall. It is worth noting that the shift from enhanced to attenuated turbulence intensity takes place at the outer end of the log layer. The location of $y^+ = 600$ is marked in Fig. 7. The turbulence energy spectra at $(y-R)/R = 0.17$, both in the case where particles are present and for the particle-free case, are shown in Fig. 8. There is an increase in the energy at low frequencies with particles while the energy levels at high frequencies are unchanged. At a position closer to the lower wall where the turbulence is damped, the spectrum shows somewhat different behaviour. Fig. 9 shows the turbulence energy spectrum at $(y-R)/R = 0.73$. Here, in the log-layer, the energy has decreased at all frequencies and the shape of the spectrum is unchanged, which gives a lower turbulence intensity. In the upper part of the pipe, the energy spectra are unchanged as compared with the spectra of the unladen flow.

For case 2 with spherical particles and a mean velocity of 19 m/s, the effects on the mean velocity profile and on the turbulence levels are less pronounced but show the same features as in case 1. Fig. 10 shows the mean velocity profiles for case 2 and for the unladen case. The profile with particles is still somewhat asymmetric, with a small decrease in the velocity below the centre and a small increase of the velocity above the centre. The profile of the turbulence intensity is shown in Fig. 11. The effect of the particles is similar to the effect in case 1. There is a small increase in turbulence intensity below the centreline of the pipe. This enhanced turbulence intensity also occurs outside the log layer, cf. Fig. 11. The reason why the decrease in turbulent energy is much smaller in this case is that the particles are more evenly distributed and that the

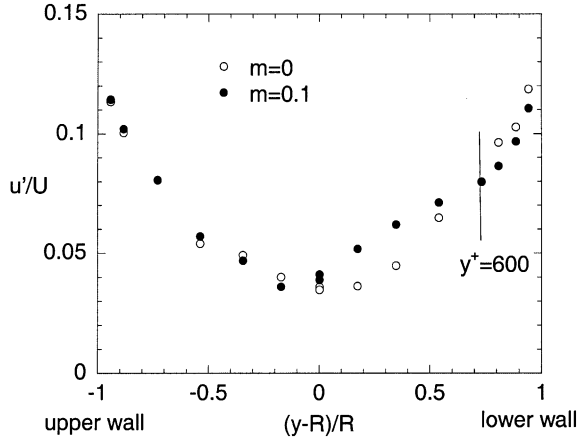

Fig. 7. Dimensionless turbulence intensity profiles for case 1 and for the unladen flow.

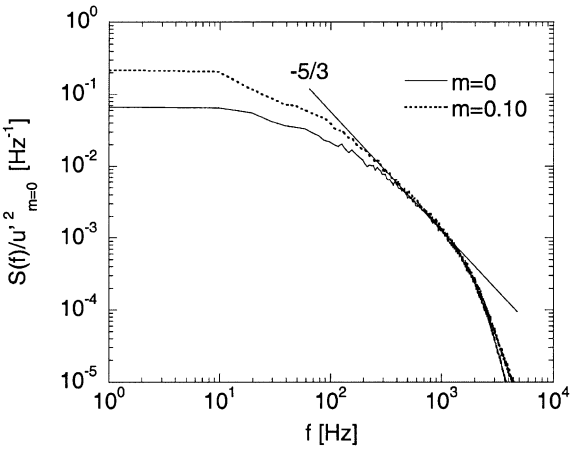

Fig. 8. Turbulent spectra at position $y = 90$ mm for case 1 and for the unladen flow.

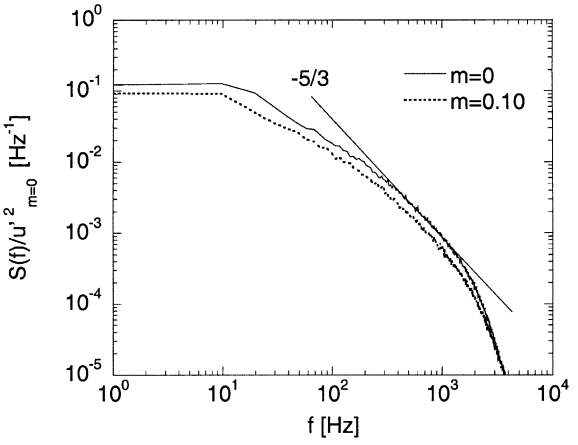

Fig. 9. Turbulent spectra at position $y = 61$ mm for case 1 and for the unladen flow.

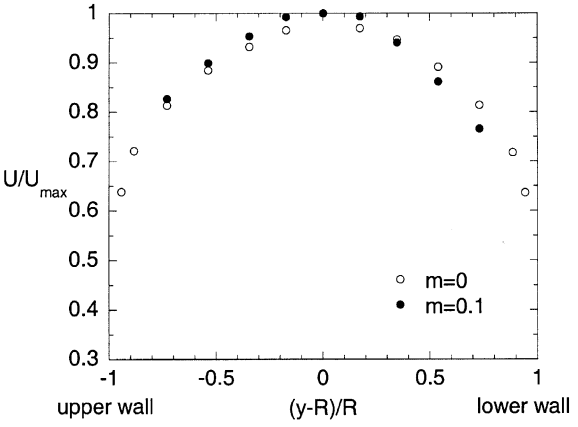

Fig. 10. Dimensionless mean velocity profiles for case 2 and for the unladen flow.

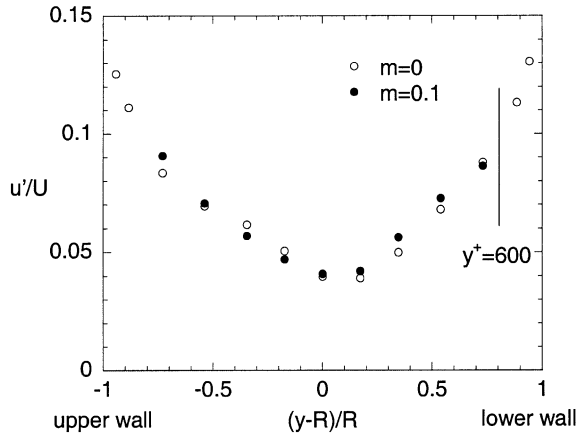

Fig. 11. Dimensionless turbulence intensity profiles for case 2 and for the unladen flow.

local concentration of particles in the lower part of the channel is lower than in case 1. This is a result of higher dispersion owing to larger turbulent velocities when the mean velocity is increased. The turbulent spectrum at $y = 70$ mm is shown in Fig. 12. The increase in turbulent energy lies mainly in the low frequency range as in case 1.

In case 3 with low-fibre concentration, $m = 0.01$, the turbulence and mean velocity profiles are not affected by the presence of fibres. This particle concentration is apparently too low to affect the flow field.

In case 4, with a loading ratio of 0.03 of pulp fibres and a mean velocity of 19 m/s, there is a significant effect on the flow field and turbulence. The effect is also somewhat different from cases 1 and 2 with the spherical particles.

Fig. 13 shows the energy spectrum at $(y - R)/R = 0.54$ for the fibre case and for the particle-free case. It shows that the turbulent energy decreases at all frequencies except for the frequencies

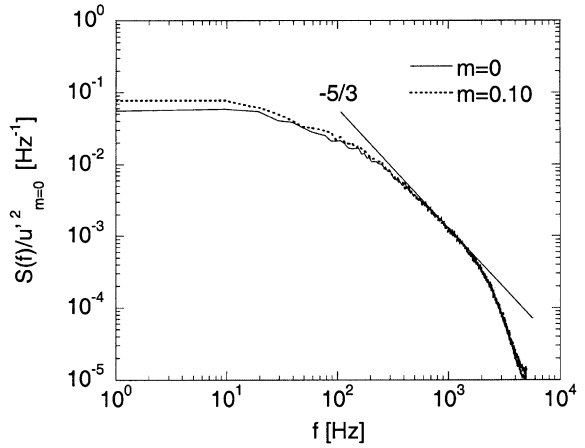

Fig. 12. Turbulent spectra at position $y = 70$ mm for case 2 and for the unladen flow.

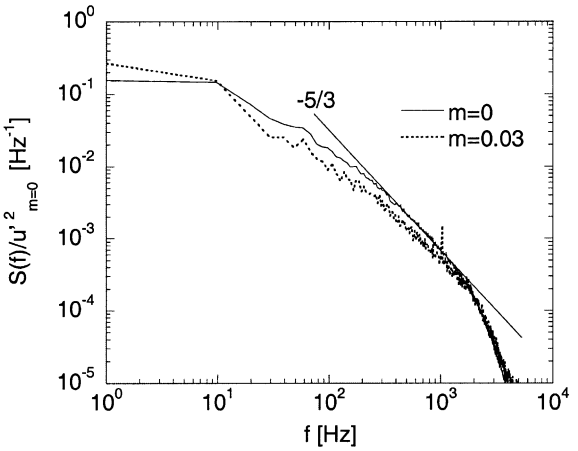

Fig. 13. Turbulent spectra at position $y = 80$ mm for case 4 and for the unladen flow.

below 9 Hz. There is a large increase at these low wave numbers, and the spectrum does not show the normal behaviour of a turbulence energy spectrum where the energy is constant at low wave numbers (below 10 Hz). Fig. 14 shows the distribution of energy at frequencies between −100 and 100 Hz for case 4 and for the unladen flow. This distribution is the averaged modulus in each frequency band of the FFT of the sampled velocity signal. It is obvious from the figure that, for the laden flow, a considerable amount of the total turbulent energy is found at zero frequency, or more precisely, in the frequency band of −4.9 to 4.9 Hz. As the energy spectrum is also the Fourier transform of the velocity auto-correlation, the zero frequency value is related to the Eulerian macroscale, cf. Tennekes and Lumley (1972). The zero frequency value observed here gives an unrealistically large macroscale for the laden flow, and the question arises whether this low frequency increase should be interpreted as turbulent fluctuations. Fig. 15 gives an example of the anemometer output voltage, which is directly related to the gas velocity, and a slow velocity

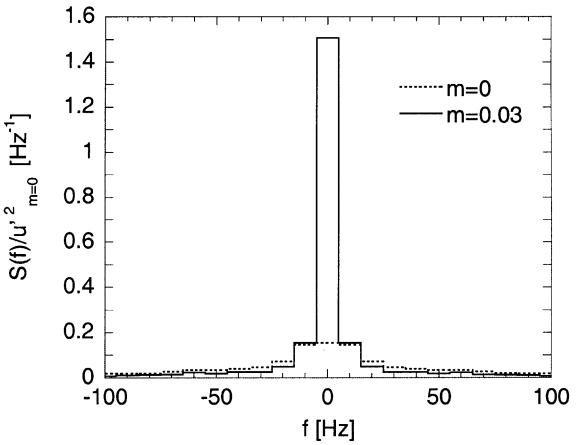

Fig. 14. Distribution of turbulent energy between −100 and 100 Hz for case 4 and for the unladen flow.

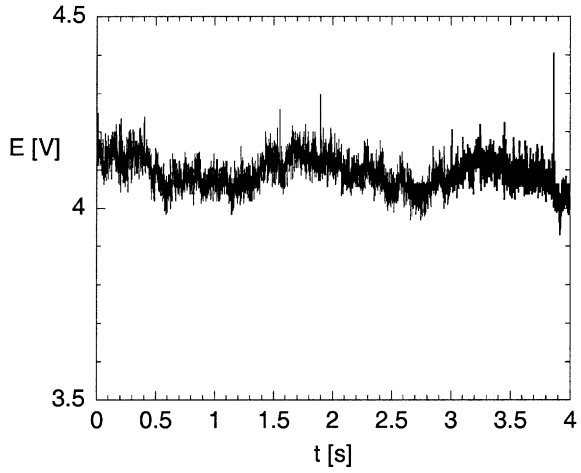

Fig. 15. An example of the sampled anemometer voltage signal in case 4.

variation is observed. The frequency of the slow variations is approximately 0.6 Hz, and the amplitude is large as compared with all other variations if the spikes caused by collisions between single fibres and the probe are excluded.

A hot film is sensitive to all velocity variations perpendicular to the probe, and it is a reasonable assumption that the low-frequency velocity fluctuations are caused by fibre flocs passing the probe. These flocs may be as large as 10–15 mm and they will generate a wake and affect the surrounding free gas mean velocity. Moreover, the floc assumption is supported by the fact that no similar effect has occurred in any of the other cases studied. Hence, when calculating the turbulence intensity, it is reasonable to digitally high-pass filter the sampled data from 10 Hz to cancel out the effect of the flocs. The method used here is of course a question of definition of turbulence as well as choice of the time interval for calculating statistical properties. Fig. 16 shows the turbulence intensity for the particle-free case and for case 4, filtered and non-filtered. For the

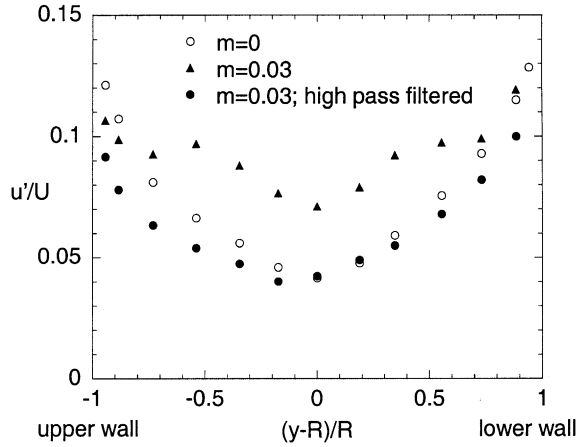

Fig. 16. Dimensionless turbulence intensity profiles for case 4, filtered and non-filtered and for the unladen flow.

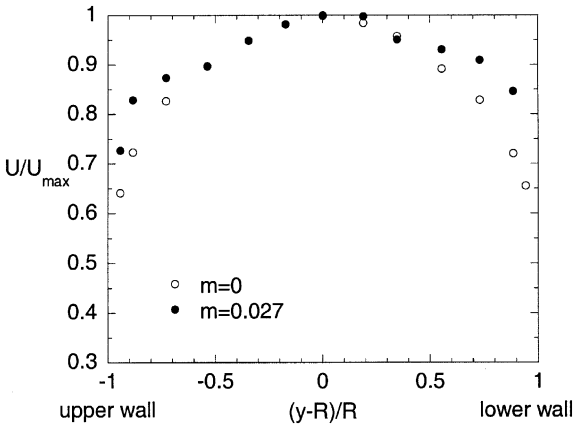

Fig. 17. Dimensionless mean velocity profiles for case 4 and for the unladen flow.

non-filtered case, the turbulence intensity increases over the entire cross-section. However, if one chooses not to regard the disturbances caused by flocs as turbulence, this intensity is severely overestimated. For the filtered case, the turbulence intensity has decreased over the entire cross-section except at the position in the centre and just below the centre of the pipe. The decrease is also somewhat larger in the upper part of the pipe than in the lower part, cf. Section 6. Fig. 17 shows the mean velocity profile, which is flattened as compared with the particle-free flow. The profile is not as smooth as in the other cases. This is because of the variations in mean velocity caused by fibre flocs passing the probe. These low-frequency variations make it necessary to increase the sampling time to attain stable values.

6. Discussion

In case 1 with loading ratio $m = 0.1$ and mean velocity 12 m/s, both reduction and increase in turbulence intensity occur. The turbulence intensity increases close to the centre of the pipe and decreases at the wall. There are generally several effects on the turbulence caused by the presence of particles. In a case with large particles, the slip velocity between the phases is larger and wake production of turbulence may occur. This can explain the increase in turbulence observed in a number of experimental investigations, cf., e.g. Hetsroni (1993). Smaller particles have a shorter response time and can follow smaller scales in the turbulence. Turbulent energy is transferred from the gas phase turbulence to the particles. This causes a reduction in the turbulence levels. In some cases, however, where the particle size can be regarded as "intermediate", the influence of the particles on turbulence may be both to increase and reduce it. This is the case in the measurements made by Tsuji et al. (1984), where turbulence intensity increases in the centre of the vertical pipe and decreases at the wall for particles with a mean particle diameter of 500 μm. In the present case the mean size of the particles is intermediate but the particles are not mono-sized. Therefore, the particles may have different effects depending on their actual size. Calculations by Ljus and Almstedt (2001) also show that the slip velocity is highest close to the centre of the pipe

where the turbulence intensity increases. Another explanation for the increase in turbulence intensity in a horizontal channel can be that the asymmetric velocity profile has a larger gradient in the middle of the channel, where the gradient is normally small. This gradient gives shear stress in the flow that causes additional production. There is also an effect of particles on the turbulent structure, i.e. the length scales of the turbulence. In the area where turbulence is enhanced, the spectra show that there is an increase in energy at low wave numbers relative to the energy at high wave numbers. This is contradictory to the results of Tsuji et al. (1984), where there is an increase at high wave numbers relative to the low wave numbers. In the present study, the energy decreases at all wave numbers at the wall and there is no redistribution between the different wave numbers caused by the particles. This means that the energy at low wave numbers increases when mainly production is increased while, when dissipation increases, the energy decreases at all wave numbers and the shape of the spectrum, i.e. the distribution of energy between different wave numbers, does not change. Note that our spectra are all normalized with the integral of the corresponding unladen spectra, i.e. variance $\overline{uu}$ for the particle-free case, in order to be able to compare the different spectra with each other. It is not obvious how the normalization should be done, and it is important to note that, depending on the normalization, the levels of the compared spectra can shift up and down. It is thus important to normalize the spectra that will be compared with the same numerical value. The same normalization has been used by Kulick et al. (1994), who made turbulence measurements and calculated spectra with 70 μm copper particles present in the airflow. Their measurements show a significant decrease in the turbulent energy levels. It is also worth noting that the 5/3 law for inertial sub-range holds for all our spectra, which was not the case for the spectra in the investigation by Kulick et al. (1994).

In case 2, with a higher velocity, the same effects on the turbulence levels and on the spectra as in case 1 can be observed but the changes are less pronounced. This is of course an effect of lower local concentration. The loading ratio is the same but, since the velocity is higher, the turbulent velocities are higher, which means that the flow can better carry the particles and the distribution of particles is more even. Because of this, there is less accumulation of particles in the lower part of the channel at higher velocity and their effect on the turbulence is much smaller.

In case 3 with the lowest loading ratio of fibres, turbulence is not affected by the presence of particles, which is in agreement with the literature, where turbulence should not be affected at particle concentrations lower than 10^{-6}, cf., e.g. Elgobashi (1994).

Case 4 is the most complicated case because the particles are fibres with large aspect ratios, i.e. the particles have one small length scale of about 50 μm and another larger length scale in the order of a few millimeters and, in addition, the fibres form flocs which might be of larger length scales, typically in the order of 10 mm. The effects on the mean velocity profile and turbulence profile indicate that the fibres are not as unevenly distributed as the spherical particles. The profiles are much more symmetric than in the spherical case. It is likely that the single fibres (not the fibre flocs) would be more evenly distributed than the spherical particles. Fibres would probably have a tendency to align along the mean velocity direction, i.e. horizontally, which gives a lift force on the fibre from both the mean velocity and the turbulence component in the radial direction. However, the flocs of fibres will probably have a greater tendency to be unevenly distributed with more flocs in the lower part of the pipe.

If the effect on the turbulence intensity is considered when the mean velocity variation is filtered out, the effect is a reduction in turbulence intensity over the whole cross-section. This is probably

the effect of single fibres that can respond to fairly high-frequency fluctuations. The flocs create low-frequency variations, which can be interpreted as turbulence or "quasi turbulence". However, as they are nearly sinusoidal, cf. Fig. 15, such an approach may be questioned as it violates the randomness of turbulence. Hence, these low-frequency fluctuations have been regarded as mean velocity variations rather than turbulence. The reduction in turbulence intensity is somewhat smaller in the lower part of the pipe where we expect the concentration to be largest. It is however likely that the single fibres that are responsible for the reduction in turbulence are fairly evenly distributed, while the flocs that cause changes in the mean velocity are concentrated in the lower part. The flocs might give rise to the production of turbulence because they create additional gradients in the mean velocity field in both the streamwise direction and across the pipe. These gradients will contribute to the production of turbulence since e.g. the production, P_{11}, of the turbulence component, $\overline{uu}$, in a cartesian coordinate system, is given by

$$P_{11} = -2\left\{\overline{uu}\frac{\partial U}{\partial x} + \overline{uv}\frac{\partial U}{\partial y} + \overline{uw}\frac{\partial U}{\partial z}\right\}. \tag{2}$$

When a floc passes the studied position, at least the first two right-hand terms in the expression above are non-zero. This contribution to production by the wake behind a particle and the vortex shedding has been modelled with several approaches, e.g. by Yuan and Michaelides (1992), Kenning and Crowe (1997) and Yokomine and Shimizu (1995).

7. Conclusions

The spherical particles cause a decrease in turbulence in the log-layer and an increase in the middle of the pipe. The turbulent energy spectra show that the increase in turbulent kinetic energy lies in the low wave number range. At the positions close to the wall, however, where turbulence decreases, the decrease is evenly distributed over all wave numbers and does not change the shape of the energy spectrum. The single fibres cause a decrease in the turbulence levels over the entire cross-section.

The fibre flocs give additional production of turbulence by creating gradients in the mean velocity. Therefore, the decrease in turbulence levels is lower below the centreline where the flocs accumulate. The fibres also have greater influence on turbulence than the spherical particles at lower particle concentrations because of the lower response time.

Acknowledgements

The authors would like to thank the Swedish Foundation for Strategic Research (SSF) and SCA Research AB for financial support of this work.

References

Abrahamsson, H., Johansson, B., Löfdahl, L., 1994. A turbulent plane two-dimensional wall jet in a quiescent surrounding. Eur. J. Mech. B 13, 533–556.

Bellhouse, B.J., Schulz, D.L., 1967. The determination of fluctuating velocity in air with heated film gauges. J. Fluid. Mech. 29, 289–295.

Chen, C.P., Wood, P.E., 1984. Turbulence closure modeling of two-phase flows. Chem. Eng. Commun. 29, 291–310.

Choi, Y.D., Chung, M.K., 1983. Analysis of turbulent gas–solid suspension flow in a pipe. J. Fluids Eng. 105, 329–334.

Dannon, H., Wolfshtein, M., Hetsroni, G., 1977. Numerical calculations of two-phase turbulent round jet. Int. J. Multiphase Flow 3, 223–234.

Elgobashi, S.E., 1994. On predicting particle-laden turbulent flows. Appl. Sci. Res. 52, 309–329.

Elgobashi, S.E., Abou-Arab, T.W., 1983. A two-equation turbulence model for two-phase flows. Phys. Fluids 26, 931–938.

Hetsroni, G., 1993. The effect of particles on the turbulence in a boundary layer. In: Roco, M.C. (Ed.), Particulate Two-phase Flow. Butterworth-Heinemann, Boston.

Kaftori, D., Hetsroni, G., Banerjee, S., 1998. The effect of particles on wall turbulence. Int. J. Multiphase Flow 24, 359–386.

Kenning, V.M., Crowe, C.T., 1997. On the effect of particles on carrier phase turbulence in gas–particle flows. Int. J. Multiphase Flow 23, 403–408.

Kulick, J.D., Fessler, J.R., Eaton, J.K., 1994. Particle response and turbulence modification in fully developed channel flow. J. Fluid Mech. 227, 109–134.

Lee, J., Crowe, C.T., 1982. Scaling laws for metering the flow of gas–particle suspensions through Venturis. Trans. ASME 104, 88–91.

Ljus, C., Almstedt, A.E., 2001. Particle transport and turbulence modification in a horizontal channel, submitted.

Ljus, C., Johansson, B., Almstedt, A.E., 2000. Frequency response method of hot-film measurements in turbulent airflow, Exp. Fluids 29, 36–41.

Löfdahl, L., Stemme, G., Johansson, B., 1992. Silicon based flow sensors used for mean velocity and turbulence measurements. Exp. Fluids 12, 270–276.

Pourahmadi, F., Humphrey, J.A.C., 1983. Modeling solid–fluid turbulent flows with application to predicting erosive wear. Phys. Chem. Hydrodyn. 4, 191–219.

Rashidi, M., Hetsroni, G., Banerjee, S., 1990. Particle–turbulence interaction in a boundary layer. Int. J. Multiphase Flow 16, 935–949.

Sato, Y., Hanzawa, K., Maeda, M., 1995. Interactions between particle wake and turbulence, in a water channel flow. In: Serizawa, A., Fukano, T., Bataille, J. (Eds.), Advances in Multiphase Flow. Elsevier, Amsterdam.

Schlichting, H., 1968. Boundary-layer Theory. McGraw-Hill, New York.

Sharma, M.P., Crowe, C.T., 1978. A novel physico-computational model for quasi one-dimensional gas–particle flows. J. Fluids Eng. 100, 343–349.

Siddal, R.G., Davies, T.W., 1972. An impoved response equation for hot-wire anemometry. Int. J. Heat Mass Transfer 14, 367–368.

Tennekes, H., Lumley, J.L., 1972. A First Course in Turbulence. The Massachusetts Institute of Technology.

Tsuji, Y., Morikawa, Y., 1982. LDV measurements of an air–solid two-phase flow in a horizontal pipe. J. Fluid Mech. 120, 385–409.

Tsuji, Y., Morikawa, Y., Shiomi, H., 1984. LDV measurements of an air–solid two-phase flow in a vertical pipe. J. Fluid Mech. 139, 417–434.

Yokomine, T., Shimizu, A., 1995. Prediction of turbulence modulation by using k–ε model for gas–solid flows. In: Serizawa, A., Fukano, T., Bataille, J. (Eds.), Advances in Multiphase Flow. Elsevier, Amsterdam.

Yuan, Z., Michaelides, E.E., 1992. Turbulence modulation in particulate flows – a theoretical approach. Int. J. Multiphase Flow 18, 779–785.